JPET Fast Forward. Published on July 15, 2014 as DOI: 10.1124/jpet.114.212779
This article has not been copyedited and formatted. The final version may differ from this version.

Perampanel, an Antagonist of α-amino-3-hydroxy-5-methyl-4-isoxazolepropionic acid (AMPA) Receptors for the Treatment of Epilepsy:

Studies in Human Epileptic Brain, Non-Epileptic Brain, and in Rodent Models[1]

R Zwart, E Sher, X Ping, X Jin, JR Sims, Jr, AS Chappell, SD Gleason, PJ Hahn, K Gardinier, DL Gernert, J Hobbs, JL Smith, SN Valli, and JM Witkin

Lilly Research Laboratories
Eli Lilly and Company
Indianapolis, Indiana USA (JMW, SNV, SDG, JRS Jr, ASC, PJH, KG, DG)
and
Windlesham, Surrey, UK (RZ, ES)

Indiana University/Purdue University
Riley Hospital
Indianapolis, Indiana USA (XP, XJ, JH, JS)

Running Title: Perampanel and AMPA Receptor Antagonism

Correspondence:
J. M. Witkin
Psychiatric Drug Discovery, Lilly Research Laboratories
Lilly Corporate Center, Indianapolis, IN 46285-0501
317 277-4470 - phone
317 276-7600 - fax
jwitkin@lilly.com

Document Statistics

Tables	2
Figures	6
Abstract	250 words

Non-Standard Abbreviations

ADD: after discharge duration

ADT: after discharge threshold

AED: antiepileptic drugs

AMPA: α-amino-3-hydroxy-5-methyl- 4-isoxazolepropionic acid

CTZ: cyclothiazide

EACSF: excitable artificial cerebral spinal fluid

GYKI 53773 = LY300164: 7-acetyl-5-(4-aminophenyl)-8,9-dihydro-8-methyl-7H-1,3 dioxolo(4,5H)- 2,3-benzodiazepine

LFP: local field potentials

PI: protective index

Abstract

Perampanel (Fycompa®) is an AMPA receptor antagonist used as an adjunctive treatment of partial-onset seizures. We asked whether perampanel has AMPA receptor antagonist activity in both cerebral cortex and hippocampus, associated with antiepileptic efficacy, and also in cerebellum, associated with motor side-effects, in rodent and human brain. We also asked if epileptic and non-epileptic human cortex is similarly responsive to AMPA receptor antagonism by perampanel. In rodent models, perampanel decreased epileptic-like activity in multiple seizure models. However, doses of perampanel that had anticonvulsant effects were within the same range as those engendering motor side effects. Perampanel inhibited native rat and human AMPA receptors from the hippocampus as well as the cerebellum that were reconstituted into *Xenopus* oocytes. In addition, with the same technique, perampanel inhibited AMPA receptors from hippocampal tissue that was removed from a patient that underwent surgical resection for refractory epilepsy. Perampanel inhibited AMPA receptor-mediated ion currents from all the tissues investigated with similar potency (IC_{50} values ranging from 2.6 to 7.0 μM). Cortical slices from the left temporal lobe derived from the same patient were studied in a 60-microelectrode array. Large field potentials were evoked on at least 45 channels of the array and 10 μM perampanel decreased their amplitude and firing rate. Perampanel also produced a 33% reduction in the branching parameter demonstrating effects of perampanel at the network level. These data suggest that perampanel blocks AMPA receptors globally across the brain to account for both its antiepileptic and side-effect profile in rodents and epileptic patients.

Since the pioneering work of Hayashi (1944; English publication 1952), it has been known that glutamate plays a prominent role in epileptic phenomena. Ion channels regulating glutamatergic and GABAergic synaptic transmission provide the dominant control over central nervous system excitability and therefore play a large role in the initiation and suppression of epileptic phenomena and represent the molecular substrate for a predominant number of currently used antiepileptic drugs (AEDs). AMPA (α-amino-3-hydroxy-5-methyl-4-isoxazolepropionic acid) receptors regulate fast excitatory neurotransmission in the mammalian nervous system and have been a target of AED discovery and development for many years. Additionally, data from genetic studies (Lerche et al., 2013) as well as AMPA receptor upregulation in brains from epileptic patients (Palomero-Gallagher et al., 2012), have added additional rationale for targeting AMPA receptors in the control of epilespy.

Multiple structurally-distinct AMPA receptor antagonists, including competitive and non-competitive blockers, have been shown to possess potent and efficacious activity in a range of in vitro and in vivo models detecting AED efficacy (Rektor, 2013; Rogawski, 2011, 2013; Russo et al., 2012). A few of these molecules have been investigated in humans for their antiepileptic potential. The AMPA receptor antagonist talampanel (GYKI 53773; LY300164) was shown to produce significant reduction in seizure frequency with dizziness (52%) and ataxia (26%) being the only adverse events reported (Chappell et al., 2002). Final proof of concept that AMPA receptor antagonism can serve as an antiepileptic control of refractory partial seizures came with the approval of the non-competitive antagonist, perampanel (Fycompa®; **Fig. 1**), which is the first selective AMPA receptor antagonist on the market.

Perampanel has demonstrated efficacy in multiple preclinical models that helped inform drug development for epilepsy (Hanada et al., 2011; Hibi et al., 2012; Rogawski and Hanada, 2013). Perampanel has been investigated in several Phase III clinical studies (French et al., 2012; Rektor et al., 2012; Krauss et al., 2012, 2013). The key clinical trials were conducted on a global level as randomized, double-blind, placebo-controlled, dose-escalation studies that examined 1,480 patients with partial-onset seizures. These studies demonstrated that perampanel as an adjunctive therapy significantly reduced seizure frequency in patients with partial-onset seizures with or without secondary generalized seizures (see reviews and analysis by Gao et al., 2013; Rheims and Ryvlin, 2013; Steinhoff et al., 2013; Zaccara et al., 2013). Fycompa® was approved (October, 2012) by the U.S. FDA for use as an adjunctive treatment of partial-onset seizures with or without secondarily generalized seizures in patients with epilepsy age 12 years and older. However, as observed with talampanel, perampanel also engenders a range of side effects predicted from both its mechanism of action and preclinical data that include dizziness, somnolence, fatigue, irritability, falls, nausea, ataxia, balance disorder, gait disturbance, vertigo, and weight gain. Nonetheless, at efficacious dosages, perampanel is generally well tolerated.

AMPA receptors are widely expressed in the central nervous system. There are four different AMPA receptor subunits (GLK_{A1-4}) and these subunits are broadly, albeit differentially, expressed in the brain. The subunit selectivity of perampanel among AMPA receptor isoforms is not known (Rogawski and Hanada, 2013). Since perampanel causes beneficial as well as side effects, we presume that perampanel inhibits AMPA receptors broadly across the brain regardless of their subunit composition. Our hypothesis

is that the beneficial effects of perampanel are mediated by AMPA receptors in brain regions related to epilepsy (cerebral cortex, hippocampus, amygdala, thalamus) and that some of the side effects are caused by inhibiting AMPA receptors in other brain regions. The cerebellum is likely to play a role in some of the side effects observed with parampanel (dizziness, falls, nausea, ataxia, balance disorder and vertigo) based upon the known physiological regulation of these clinical signs by the cerebellum (Della-Morte and Rundek, 2012; Salman, 2002). The hypothesis was tested with novel electrophysiological techniques to study the sensitivity to perampanel of AMPA receptors from different brain areas of both rat and human. In addition, since epileptic brain tissue has shown changes in AMPA receptor density (c.f., Brines et al., 1997; Palomero-Gallagher et al., 2012), we also evaluated the effects of perampanel in human epileptic brains.

In particular, we adopted a recently developed technique (Miledi et al., 2006; Eusebi et al., 2009) based on the reconstitution of native human neurotransmitter receptors into oocytes of the African clawed toad (*Xenopus laevis*), followed by voltage-clamp recording. The strength of this technique is that it can be applied to post-mortem frozen human brain samples as well as freshly-excised tissue. The technique can also be used to study native ion channels from diseased brain. For example, it has been applied to study differences in native human $GABA_A$ receptors between control and epileptic human hippocampi (Palma et al., 2005; Palma et al., 2007).

Finally we examined the effects of perampanel directly on fresh cortical slices obtained from the same epileptic patient studied in oocytes, but this time utilizing a 60 microelectrode recording array (Hobbs et al., 2010).

JPET Fast Forward. Published on July 15, 2014 as DOI: 10.1124/jpet.114.212779
This article has not been copyedited and formatted. The final version may differ from this version.

Methods

Rodent behavioral assays

Animals. Male Sprague Dawley rats (Harlan Sprague Dawley. Indianapolis, IN), weighing 90-110 grams at the time of test were used. Animals were housed 5 per cage with *ad libitum* food and water in a large colony room with a standard light cycle (lights on 6am, lights off 6pm). F344 (Harlan Sprague Dawley. Indianapolis, IN) were used for the studies of i.v. pentylenetetrazole infusion. Male CD1 mice (Taconic Farms) weighing 23-31g were used. Animals were maintained in the colony room for at least 3 days before testing. Animals were moved to a quiet room 1 hour prior to the start of the test. All studies were performed according to the guidelines set forth by the National Institutes of Health and implemented by the Animal Care and Use Committee of Eli Lilly and Company.

Electroshock. Mice (n=10/dose) were used with Wahlquist Model H stimulator with 0.2 sec stimulation with corneal electrodes. Mice were observed for approximately 10 sec after administration of the electrical stimulus (10uA) and the types of convulsions were recorded (0 = no convulsion, 1 = clonus, 2 = tonic flexion, 3 = tonic extension). Mice were euthanized immediately following test. Only one mouse was used per treatment. Tonic extension was used as the primary endpoint for calculation of ED_{50} values.

Inverted Screen Test. Prior to dosing rats or mice with PTZ, the animals were tested (30 min post drug administration) on an inverted screen. The apparatus is made of six 11cm x 14 cm (mouse) or four 13cm x 16 cm squares (rat) of round hole, perforated

stainless steel mesh (18 holes/square inch, 3/16 inch diameter, ¼ inch staggered centers, 50% open area) which are mounted 15 cm apart on a metal rod, 35 cm above the table top.

For mice, on the day prior to test, mice are placed on the screen and the rod is rotated 180° over 2-3 seconds. The amount of time it takes for the test subject to climb to the top of the screen is recorded. For test subjects that hang on the bottom for the maximum of 60 sec, a 60 sec score is recorded. Test with compound on board is studied the following day in the same manner.

For rat studies, animals were dosed with test compound, po, and returned to their home cage. Twenty five min after pre-treatment, animals were tested on the inverted screen and were scored after 60 seconds as follows: (0=climbed over, 1= hanging on to screen, 2= fell off). After the inverted screen test, animals were dosed with pentylenetetrazol (PTZ) in a volume of 1 ml/kg and placed in an observation cage (40.6x20.3x15.2 cm) with a floor containing 0.25 inches of wood chip bedding material.

Pentylenetetrazole (PTZ)-Induced Seizures. Drugs were studied for their ability to prevent or dampen seizures induced in mice or rats after s.c. PTZ dosing. Animals were than observed for 30 min post PTZ for clonus (defined as clonic seizure of fore- and hindlimbs during which the mouse demonstrated loss of righting) or for tonic seizures as exemplified by loss of righting accompanied with tonic hindlimb extension. The dose of PTZ used in the rat studies was 35 mg/kg, s.c., and the dose in mice was 70 mg/kg, i.p., based upon estimated ED_{90} values for PTZ in these assays.

Pentylenetetrazole (PTZ)-Induced Seizure Threshold. The threshold dose of PTZ to produce seizures was measured in rats with and without perampanel pretreatment

during i.v. PTZ infusion. Male F-344 Harlan rats were randomly assigned to treatment groups and dosed with vehicle or test compound. After the appropriate pretreatment time as noted above, rats were placed in a restrainer and a winged infusion needle was inserted into the lateral tail vein. Intravenous infusion with 10 mg/ml PTZ at a rate of 0.5 ml/min then was initiated until a clonic convulsion occurs and the time to clonic convulsion is recorded in sec or a maximum of 4 minutes, 240 seconds is recorded. Following infusion, rats are euthanized. The dose of PTZ required to elicit a clonic convulsion was calculated using the infusion rate, concentration of PTZ, time to clonic convulsion, and animal weight.

Basolateral Amygdala Kindling. Drugs were evaluated for their ability to impact seizure parameters in rats that were fully kindled by daily electrical stimulation of the amygdala of rats. The electrical kindling equipment consisted of a computer connected to an amplifier (ISASI Quad Amplifier from Astro-Med Inc.GRASS Model 15RX). The amplifier was connected to a maximum of two telefactor units (GRASS Telefactor W MOID S88). Each telefactor unit is connected to a maximum of two battery units (Photoelectric Stimulator Isolation Unit Constant Current Output). Each battery unit is then connected to one shock chamber. Valproic acid was used as a positive control. A bipolar electrode for electrical stimulation and EEG recording is stereotaxically implanted into one hemisphere of the basolateral amygdala (AP -2.2 , ML -4.8, DV -8.5 mm, relative to bregma) of male Wistar rats. After post-operative recovery, electrical kindling begins, where a subthreshold constant current (400µA, 1 ms, monophasic square-wave pulses, 60 Hz for 1 sec) is given once a day Monday-Friday for about 4-6 weeks until a rat is fully kindled. A fully kindled rat has experienced 10

consecutive stage 5 seizures or 10 of its last 12 were stage 5 according to the Racine Scale.

Twelve fully kindled rats were assigned to this study and eight rats were selected and randomized to initial compound treatment groups from baseline after discharge threshold (ADT), seizure severity score, and after discharge duration (ADD). A pseudo within-subjects Latin Square design was used for subsequent testing, as replacement rats were used in the event that an assigned rat did not meet the pre-compound testing baseline criteria or a rat lost it head cap during a seizure. On test day rats were dosed 30 min prior to beginning stimulation. After the pre-treatment, rats were stimulated using an ascending staircase sequence beginning at 10μA and increasing in log unit steps of 10, 16, 25, 40, 65, 100, 160, 250, and 400μA. Animals were stimulated until they were assigned a Seizure Severity Score for a visually observably seizure or they reached the 400μA threshold limit. ADD was determined following testing. ADT was the current that induced a scoreable seizure. *Seizure Severity*: Racine score of behavioral response to stimulation: 0 = no behavioral response; 1 = immobility, staring and/or facial clonus; 2 = head nodding, jaw clonus, and/or tongue protrusion; 3 = unilateral forelimb clonus; 4 = bilateral forelimb clonus and/or rearing; 5 = bilateral forelimb clonus with rearing and loss of balance. After-Discharge Duration (ADD) is the duration of the first after-discharge.

Statistics anaylsis. ADT, ADD, and seizure severity scores were recorded for each animal. Data was analyzed by ANOVA and post-hoc Dunnett's *t*-test. Statistical analyses were performed using JMP statistical software (SAS Institute Inc., Cary, NC). A probability of $p \leq 0.05$ was used as the level of statistical significance.

Compounds. Perampanel [2-(2-oxo-1-phenyl-5-pyridin-2-yl-1,2-dihydropyridin-3-yl)benzonitrile hydrate 4:3] (Fig. 1) was synthesized by Eli Lilly and Company. The other compounds were obtained from commercial suppliers: Lacosamide (10 mg/ml) (UCB, Smyrna, GA USA), diazepam (Sigma-Aldrich, St. Louis, MO, USA), Valproic acid Na (Sigma-Aldrich, St. Louis, MO, USA), pictrotoxin, and pentylenetetrazole (Sigma-Aldrich, St. Louis, MO, USA). Perampanel was suspended in 10% acacia and 0.05% Dow anti-foam in a volume of 10 ml/kg for both rat (administered via PO route, 30 minutes prior to testing) and mouse (administered 30 min via IP route) studies. Lacosamide was diluted from a stock solution of 10 mg/ml with saline (0.9% NaCl) and dosed in a volume of 1 or 3 ml/kg for rat (dosed via IP route, 30 min prior to testing) and a volume of 10 ml/kg was used for mice (dosed via IP route, 30 min prior to testing). Diazepam was dissolved in 20% 2-hyroxypropyl-beta-cyclodextrin in water. Diazepam was administered in a volume of 1 ml/kg for rat (dosed via IP route, 30 min prior to testing and a volume of 10 ml/kg was used for mice (dosed via IP route, 30 min prior to testing). Valproic acid was dissolved in saline and administered in a volume of 4 ml/kg to rats via IP route, 30 min prior to testing and dosed as the acid form.

Xenopus Oocyte Studies: Effects on human and rat hippocampal and cerebellar AMPA receptors reconstituted into _Xenopus_ oocytes.

Rat hippocampal and cerebellar brain samples were taken from 2-3 months old male Sprague Dawley rats (Charles River, Margate, U.K.). Frozen fragments of human hippocampal and cerebellar brain samples were obtained from Asterand (Detroit, U.S.A.) and kept frozen at -80°C. Transport of the human tissue samples from the USA to the UK

took place on dry ice. Both human brain samples were from the same donor, a 67 year old Caucasian male whose cause of death was cardiac arrest. During his life the donor's height was 172 cm, weight was 74 kg, BMI (Body Mass Index) was 25.0, and he was clinically diagnosed with hypertension, chronic pulmonary disease and hyperlipidemia. He was on the following medications: unspecified inhalers, unspecified statins and Vicodin. The excision of the tissues took place in 2010 and the post-mortem intervals were 723 min (hippocampal tissue) and 758 min (cerebellar tissue). Membrane preparations of the frozen human tissues were made on the 4th of August 2011.

Membrane preparations were also made from hippocampus obtained from a 13-year-old male patient undergoing surgical resection for refractory epilepsy. This tissue was resected, prepared, and utilized in accordance with an IRB (0612 Indiana University School of Medicine, Indianapolis, IN) and approval from the parent of the patient was obtained prior to surgery. The patient voluntarily elected to be in the study. Cortical tissue was harvested from left temporal lobe in an area with the most active epileptogenic profile of the patient's seizure focus as identified by preoperative video electroencephalography and intraoperative electrocorticography. A 2 x 2 mm piece of cortex within the seizure focus was removed immediately after the intraoperative electrocorticography; removal took less than 30 seconds. Cerebral vasculature was left intact as the tissue was resected and immediately placed for 3 min in ice-cold artificial cerebrospinal fluid (ACSF) containing in mM: Sucrose 125, KCl 3, $NaH_2PO_4*H_2O$ 1.25, $NaHCO_3$ 26, $MgSO_4*7H_2O$ 2, $CaCl_2*2H_2O$ 2, D-glucose 10, saturated with 95% O_2/5%CO_2.

Membrane preparations from these tissues were prepared according to the method developed and described by Miledi et al. (2006) and Eusebi et al. (2009). In short: 0.1 – 0.5 g of fresh rat tissue or of frozen human tissue was homogenized in ice-cold glycine buffer (in mM: 200 glycine, 150 NaCl, 50 EGTA, 50 EDTA, 300 sucrose) to which 10 µl protease inhibitor cocktail (Sigma) was added per ml glycine buffer. The homogenate was centrifuged at 4°C for 15 min at 9500 g. The supernatant was subsequently centrifuged at 4°C for 2 hrs at 100,000 g with an ultra-centrifuge and the pellet was re-suspended in ice-cold assay buffer (5 mM glycine). The protein concentration of the membrane preparations were measured using the Pierce BCA protein assay kit (Thermo Scientific, Rockford, IL, U.S.A.) and were between 2.5 and 7 mg/ml. Aliquots of the suspensions were kept at -80°C and were thawed just before injection into *Xenopus* oocytes.

Xenopus oocytes (stage V-VI) were removed from schedule I sacrificed frogs and defolliculated after treatment with collagenase type I (5 mg/ml calcium-free Barth's solution) for 1.5. h at room temperature. 60 nl of membrane suspension was injected per oocyte using a Drummond (Broomall, PA, U.S.A.) variable volume microinjector. After injection, oocytes were incubated at 18°C in a modified Barth's solution containing 88 mM NaCl, 1 mM KCl, 2.4 mM $NaHCO_3$, 0.3 mM $Ca(NO_3)_2$, 0.41 mM $CaCl_2$, 0.82 mM $MgSO_4$, 15 mM HEPES and 50 mg/l neomycin (pH 7.6 with NaOH; osmolarity 235 mOsm). Experiments were performed on oocytes after 2-5 days of incubation. Oocytes were placed in a recording chamber (internal diameter 3 mm), which was continuously perfused with a saline solution (115 mM NaCl, 2.5 mM KCl, 1.8 mM $CaCl_2$, 1 mM $MgCl_2$, 10 mM HEPES, pH 7.3 with NaOH, 235 mOsm) at a rate of

approximately 10 ml/min. Dilutions of drugs in external saline were prepared immediately before the experiments and applied by switching between control and drug-containing saline using a BPS-8 solution exchange system (ALA Scientific Inc., Westbury, NY, U.S.A.). Between responses oocytes were washed for 2 min. Oocytes were impaled by two microelectrodes filled with 3 M KCl (0.5 – 2.5 MΩ) and voltage-clamped using a Geneclamp 500B amplifier (Axon Instruments, Union City, CA, U.S.A.) according to the methods described by Stühmer (1998). The external saline was clamped at ground potential by means of a virtual ground circuit using an Ag/AgCl reference electrode and a Pt/Ir current-passing electrode. The membrane potential was held at -60 mV. The current needed to keep the oocyte's membrane at the holding potential was measured. Membrane currents were low-pass filtered (four-pole low-pass Bessel filter, -3 dB at 10 Hz), digitized (50 Hz), and stored on disc for offline computer analysis. Data are expressed as mean ± s.e.m. All experiments were performed at room temperature.

For antagonist concentration-inhibition curves, ion currents were evoked by switching from control solution to a solution containing 100 μM AMPA and 100 μM cyclothiazide (CTZ). After 30 s of AMPA/CTZ perfusion the solution was switched to AMPA/CTZ plus various concentrations of perampanel for 20 s. The amount of inhibition was calculated from the current amplitude at the end of perampanel application and the current amplitude of the AMPA/CTZ response just before perampanel application. Concentration-inhibition curves were fitted according to the Hill equation. Curve fitting was performed using Graphpad Prism 3.01 software (San Diego, CA, U.S.A.).

Human Epileptic Cerebral Cortex Electrophsyiology.

Tissue preparation and recording: The block of tissue from the patient describe above was then sliced into coronal sections with a thickness of 250 µm using a vibratome tissue slicer. Coronal sections were cut using white matter as landmark. After cutting, slices were bathed for ~1hr at room temperature in ACSF with the same ingredients as listed above, but with 125 mM NaCl substituted for 125 mM sucrose to restore Na^{+} and allow cells to fire action potentials again.

In preparation for recording, slices were adhered to microelectrode arrays (MEA; Multichannel Systems, Reutlingen, Germany) with a solution of 0.1% polyethelinamine that had been previously applied and let to dry for 2 hrs (Wirth and Luscher, 2004). We attempted to place the tissue so that neocortical layers I-V covered the array. Slices were maintained thermostatically at 37° C and were perfused at 1.0 ml/min first with normal (NACSF) for one hour to see if the tissue was spontaneously active. If spontaneous activity did not develop after one hour the tissue was bathed in excitable ACSF (EACSF) solution containing 5 mM KCl and 0 mM Mg^{+2}. These external ionic concentrations are known to produce robust local field potential (LFP) activity in cortical brain slices (Schiff et al., 1994; Wu et al., 1999 and verified in cortical tissue from human's by Hobbs et al., 2010). Tissue was then recorded in EACSF with a concentration of 10µM of Picrotoxin for more than 1 hour. Subsequently, tissue was recorded in EACSF with a concentration of 10µM of Picrotoxin with perampanel and recorded for 1 hour. Following the perampanel addition, tissue was recorded in a washout solution of EACSF and 10 µM Picrotoxin for 1 hour.

Electrode arrays. Recordings were performed on microelectrode arrays purchased from Multichannel Systems (Reutlingen, Germany). Each array had 60 electrodes, and each electrode was 30 µm in diameter, and 30 µm high. Electrodes were arranged in a square grid with 200 µm spacing between electrodes.

Local field potential (LFP) detection. Extracellular activity from slices was recorded in the same manner as previously reported (Tang et al., 2008). Activity was sampled from all 60 electrodes (Fig. 3B) at 1 kHz and amplified before being stored to disk for offline analysis. Local field potentials (LFPs) that showed sharp negative peaks below a threshold set at 3 standard deviations of the signal were marked, and the time of the maximum excursion was recorded as the time of that LFP. Time points were binned at 4 ms resolution, as this was previously shown to match the average time between successive LFP events across electrodes (Beggs and Plenz, 2003).

In characterizing network activity, we closely followed the methods first described in (Beggs & Plenz, 2003, 2004). An avalanche is a sequence of consecutively active frames that is preceded by a blank frame and terminated by a blank frame. The length of an avalanche is given by the total number of active frames and the size of an avalanche is given by the total number of electrodes activated during the avalanche.

Measuring the branching parameter. The branching parameter, symbolized by σ, is the average number of descendant electrodes produced by a single ancestor electrode. By ancestor electrode, we mean an electrode on the array that experienced a supra-threshold LFP signal at a given time step. By descendant electrode, we mean an electrode on the array that experienced a supra-threshold LFP signal one time step after the activity

JPET Fast Forward. Published on July 15, 2014 as DOI: 10.1124/jpet.114.212779
This article has not been copyedited and formatted. The final version may differ from this version.

of the ancestor electrode. The branching parameter is straightforward to approximate from experimental data, and can be obtained by taking the parameter:

$$\sigma = \left\langle \frac{N_{2:L}}{N_{1:(L-1)}} \right\rangle,$$

where L is the length of each avalanche, N2:L is the total number of electrodes activated in frames 2 to L, N1:(L-1) is the total number of electrodes activated in frames 1 to L-1, and the angled brackets indicate averaging over all avalanches. From this definition, it is clear that the branching parameter is a measure of collective excitability in the network. Intuitively, when $\sigma < 1$, activity is damped and will quickly die out. When $\sigma = 1$, the network is in the critical state and long chains of neural activity can occur without unstable expansion. When $\sigma > 1$, activity is amplified every time step, eventually leading to excessive network activity. Excessive network activity can be induced by washing the slice in 10 uM of pictrotoxin. This increase in network activity can mimic a seizure state in the slice. Once an excited state is induced, the effects that perampanel has on network activity can be measured by the branching parameter as just described.

Results

In Vivo Studies.

Electroshock. Both perampanel and diazepam potently and fully prevented the tonic extension induced by electroshock in mice after i.p. dosing (**Table 1**).

Inverted Screen Test. The potencies of perampanel and lacosamide to disrupt behavior of mice or rats on the inverted screen test are shown in **Table 1**. Both compounds produced motoric side-effects as measured by this assay.

Pentylenetetrazole (PTZ)-Induced Seizures. Both perampanel and lacosamide were fully effective in attenuating PTZ-induced clonic seizures in both mice and rats. The potencies of these drugs under these assays are shown in **Table 1**.

Pentylenetetrazole (PTZ)-Induced Seizure Threshold. Perampanel was not effective in increasing PTZ seizure latency when dosed orally. At the highest dose tested the dose of PTZ inducing seizures was 41.7 $\pm$ 4.2 mg/kg compared to 35.1 $\pm$ 1.0 mg/kg after vehicle dosing. In contrast, the positive control in this study, valproate (300 mg/kg, i.p.), increased the threshold dose of PTZ to 86.8 $\pm$ 9.4 mg/kg. Diazepam had minimal effective dose of 0.3 mg/kg, i.p. At this dose, the threshold dose of PTZ required for seizures was 43.4 $\pm$ 0.3 mg/kg (vehicle = 37.8 $\pm$ 1.2 mg/kg PTZ).

Amygdala Kindling. In amaygdala kindled rats, perampanel and lacosamide were studied after doses of 3-30 mg/kg, p.o. Under these conditions, perampanel was efficacious in dampening all measured parameters of seizure kindling at 30 mg/kg except the after discharge duration which was also unaffected by lacosamide (**Table 1**). Although lacosamide was ½-log dose more potent in protecting against after-discharge

JPET Fast Forward. Published on July 15, 2014 as DOI: 10.1124/jpet.114.212779
This article has not been copyedited and formatted. The final version may differ from this version.

threshold and seizure severity than perampanel, it was less potent in altering convulsions driven by 400μA (**Table 1**).

Protective Indicies. When comparing potencies of perampanel on a measure of motor deficit (inverted screen) to its anticonvulsant potencies, a protective index can be calculated as Potency inverted screen/Potency Anticonvulsant. PI values > 1 indicate a margin between efficacy and side-effect doses; PI values $\leq$ 1 indicate that side-effects and efficacy are not dissociable. For PTZ clonus in rat and for the after discharge threshold measure of amygdala kindling, the PI = 0.36 and 0.13, respectively. For locosamide, estimates of the PI for these same anticonvulsant endpoints were ~0.15 and 0.3, respectively. In mice, perampanel had a PI of 0.44 in the PTZ clonus measure and 3.5 in the electroshock measure. Lacosamide had a PI estimate of ~1 for PTZ clonus in mice.

Effects on native human and rat hippocampal and cerebellar AMPA receptors reconstituted into *Xenopus* oocytes.

Oocytes injected with membranes from rat or human hippocampal or cerebellar membranes did not respond to 100 μM AMPA with measurable currents (not shown), but when 100 μM AMPA was co-applied with 100 μM of the AMPA receptor potentiator cyclothiazide (CTZ), AMPA receptor-mediated ion currents were clearly observed, which were almost completely inhibited when 30 μM perampanel was applied during the AMPA/CTZ response (**Fig. 2A**). Perampanel induced concentration-dependent inhibition of AMPA/CTZ (**Fig. 2B**). The IC_{50} and Hill-slope values are shown in **Table 2**. The data

demonstrate that perampanel inhibited native rat and human hippocampal and cerebellar AMPA receptors with similar potency and to the same extent.

Membranes were also prepared from the hippocampal tissue obtained from the epileptic patient and further injected into oocytes. Also in this case perampanel produced a concentration-dependent blockade of ion currents evoked by application of AMPA/CTZ (**Fig. 3**) with an IC_{50} of 6.7 μM, demonstrating that perampanel is indeed blocking AMPA receptors in the diseased brain.

Human Epileptic Cerebral Cortex Electrophysiology.

Characterizing multi-electrode activity. In characterizing network activity, we closely followed the methods first described in (Beggs & Plenz, 2003, 2004) and illustrated in **figure 4**. The configuration of active electrodes during one time step is called a frame.

An avalanche is a sequence of consecutively active frames that is preceded by a blank frame and terminated by a blank frame. The length of an avalanche is given by the total number of active frames and the size of an avalanche is given by the total number of electrodes activated during the avalanche.

Spontaneous activity in human slices. As reported previously human slices are rarely active in NACSF (Hobbs et al. 2010). This was also true in this experiment, and in order to test the effects of perampanel in this experiment, the slice was bathed in 10 μM of picrotoxin, elevated K^+ and reduced Mg^{2++}. This concentration was found to evoke large field potentials on at least 45 channels of the array.

Event size distributions. We commonly observed local field potentials (LFPs) that exceeded the threshold on multiple electrodes in the same time bin. We also observed cascades of consecutively active time bins (**Fig. 4**). After cascades were recorded over 45 minutes or more, it was possible to plot their size distribution. We previously reported that in data collected from rats, this size distribution had a very long tail that approached a power law (Tang, et al 2008). This distribution was not expected by chance (Beggs, 2008), but was similar to that produced by computational models of sand pile avalanches (Bak, 1996).

Perampanel effects on epileptic human brain tissue. We first recorded the slice activity for 1 hr in 10μM of Picrotoxin to establish a base line. The average amplitude was -23.34 $\pm$ 7.07 μV and the average firing rate (**Fig. 5A**) was 0.14 $\pm$ 0.02 Hz during this recording. In the second hour of recording, 10μM of perampanel was added along with the 10μM of Picrotoxin. The amplitude showed a trend toward a decrease as shown in Fig. 6A to -21.22 $\pm$ 5.24 μV and the average firing rate decreased to 0.06 $\pm$ 0.01 Hz (**Fig. 5A**). Both of these decreases were statistically significant ($p < 0.05$, paired test). This decrease in activity was maintained after washout with 10μM picrotoxin -19.68 $\pm$ 8.57 μV; and 0.06 $\pm$ 0.01 Hz (N3 reference table 1). Statistically significant decreases in both amplitude and firing rate establish that perampanel decreases activity in the slice from a human epileptic patient. Epilepsy is a network phenomenon; groups of neurons exhibiting abnormal electrical activity. Understanding epilepsy thus requires scrutiny of the activation of groups of neurons at the network level. In order to establish the effects of perampanel at the network level, we measured the branching ratio (as discussed in the methods section).

JPET Fast Forward. Published on July 15, 2014 as DOI: 10.1124/jpet.114.212779
This article has not been copyedited and formatted. The final version may differ from this version.

Branching Parameter. As previously mentioned in the methods section, 10 μM picrotoxin was washed into the slice bath to induce excitability in the slice network. After recording this picrotoxin induced excitability for 1 hour, 10 μM perampanel was washed into the slice bath while maintaining the 10 μM picrotoxin solution. The perampanel at 10 μM significantly decreased the branching ratio in the network (as data are non-normally distributed we use the Kolmogorov Smirnov paired t-test at $p< 0.05$). In **figure 6**, the tissue in 10 μM of pictrotoxin had an average branching parameter of 0.36. The addition of 10 μM of perampanel decreased the average branching parameter to 0.24 which was statistically significant at $p< 0.05$. The branching parameter continued to decrease after washout in 10μM of Picrotoxin to 0.16.

Discussion

In the present study we document that in rodent models, seizures in both rats and mice were well controlled by perampanel. Previous preclinical reports have documented efficacy for perampanel against seizures in rodents (Hanada et al., 2011; Rogawski and Hanada, 2013). In these studies, perampanel attenuated audiogenic, electroshock-induced, PTZ-induced seizures, 6 Hz-driven seizures and amygdala kindled-seizures in rodents (Hanada et al., 2011). The present findings provide the first systematic replication of the preclinical findings from Eisai Corporation (Hanada et al., 2011) that markets perampanel. The translational value of these data are documented in the correspondence in the efficacy in rodents and the antiepileptic efficacy in epileptic patients with partial-onset seizures with or without secondary generalized seizures (see reviews and analysis by Gao et al., 2013; Rheims and Ryvlin, 2013; Steinhoff et al., 2013; Zaccara et al., 2013).

In addition to anticonvulsant protection in rodents, perampanel induced motor deficits on the inverted screen test in mice and rats. The potencies for inducing motor impairments were greater than that for efficacy as an anticonvulsant with the exception of mouse electroshock seizures where a protective index of ≥ 1 was found (3.5). Low dose margins of efficacy over motor effects have been reported before in rodents (Hanada et. al., 2011). Although well tolerated, perampanel has shown motor impairments in human studies and in Phase 3 data (French et al., 2012; Rektor et al., 2012; Krauss et al., 2012, 2013). Thus, although protective indicies in rodents are not always fully translatable into human motor side-effect liabilities (Löscher and Nolting, 1999), the data with

perampanel in the current study and in Hanada et al. (2011) have uncovered the dose-dependent motor consequences of perampanel in humans.

As a first step in understanding the molecular basis of perampanel efficacy, as well as motoric effects, we explored perampanel pharmacological effects in native rodent and human preparations. With the aid of the innovative technique of reconstituting native neurotransmitter receptors into *Xenopus* oocytes we were able to demonstrate that perampanel inhibits native rat and native human AMPA receptors from both the hippocampus and the cerebellum. In addition, direct measurements from human epileptic cortical brain slices, showed that perampanel decreased amplitudes and firing rates of large evoked field potentials. These findings are important, because the inhibition of cortical and hippocampal AMPA receptors in human tissues provides an explanation for the beneficial effects of perampanel in epileptic patients.

Our results showing that perampanel also inhibits native hippocampal AMPA receptors from a refractory epileptic patient (both in oocytes and in fresh slices) show, for the first time, that perampanel acts on AMPA receptors in epileptic human brain tissue and that the AMPA receptors in the diseased state are still sensitive to the drug, a finding consistent with the antiepileptic efficacy of perampanel.

Some aspects of the fresh brain slice experiments are worth considering in more detail. Our data extend previous findings obtained with perampanel in cultured cortical neurons (Hanada et al., 2011) and studying synaptic transmission in hippocampal slice preparations of rat brain (Ceolin et al., 2012). As previously reported, tissue from humans is rarely spontaneously active in vitro (Hobbs et al. 2010). Picrotoxin acts as a noncompetitive antagonist for $GABA_A$ receptor chloride channels, and is well known for

increasing excitability in neural tissue (Mackenzie et al 2002) and was used to investigate the effects of perampanel. The results from these in vitro studies, consistently with the Phase III efficacy data,show that perampanel provides seizure protection in cortical slices from the active region of the left temporal lobe from a medication-unresolved epilepsy patient. Perampanel significantly dampened local population activity and network activity in human tissue from an epileptic patient. This conclusion was derived from three specific measures: firing rate, amplitude, and the branching parameter, all of which decreased when 10μM of perampanel was washed into the slice bath.

Although these results are statistically significant, caution must be exercised when extrapolating these findings to human tissue *in vivo.* Experiments with slices are limited by several factors. Long-range neuronal connections are severed and severing these long-range connections alters network properties, and activity in the network failed to recover and return to baseline after perampanel was washed out. As obtaining human tissue is rare, this study relies on a sample of one, and replication is warranted. Finally, in a previous publication (Hobbs et al. 2010) we showed that large network-wide events occurred simultaneously for extended periods of time in some tissue from human patients with epilepsy, and that the branching parameter was positively correlated with firing rate in these recordings. We also showed that this “seizure-like” activation can drive down the branching parameter (Hobbs et al. 2010) as the descendant of an extended network-wide event can at most have the same size, or more likely fewer branches than its ancestor. In order to confirm that the effects on the branching parameter were not derived from network-wide activation, we searched for sustained network-wide events on

time scales of up to 50s and determined that this type of activation did not decrease the branching parameter.

Finally, it is crucial to understand the source of perampanel's side effects, in order to be able to develop AEDs with better margins of safety. Given the motor impairments observed in rodents (Hanada et al., 2011; Rogawsky and Hanada, 2013; present study) and the ataxia and dizziness reported in epileptic patients at higher doses of perampanel (French et al., 2012; Rektor et al., 2012; Krauss et al., 2012, 2013), it is suggested that cerebellar AMPA receptor blockade is a primary mediator of the main side effects of perampanel. Our results, showing that both rodent and human cerebellar AMPA receptors are equally inhibited by perampanel, further corroborate this hypothesis.

We hypothesize that the optimal AMPA receptor antagonist to be used as an AED would block AMPA receptors in affected brain regions (cerebral cortex, hippocampus, amygdala, thalamus) while leaving AMPA receptors in other brain regions (e.g. cerebellum) unaffected. It is conceivable that the subunit composition of AMPA receptors in the cerebellum differ from AMPA receptors in other brain regions. If that is the case the possibility to develop subunit-selective AMPA receptor antagonists can be explored. AMPA receptor structure and function is further affected by proteins associated with AMPA receptors, like the transmembrane AMPA receptor associated proteins (TARPs). TARPS are known to influence the pharmacological properties of AMPA receptors (Menuz et al., 2007; Cokic and Stein, 2008; Kato et al., 2010). It is currently not know if the activity of perampanel is influenced by TARPs. TARP γ2 is highly expressed in the cerebellum (Tomita et al., 2003). Thus, an AMPA receptor antagonist that has reduced potency and/or efficacy at AMPA receptors associated with TARP-γ2

relative to other AMPA receptor isoforms might provide antiepileptic control without the cerebellar-mediated motor side effects.

In conclusion, our experimental findings confirm our hypothesis that peramapel antagonizes AMPA currents in both brain areas responsible for epileptic discharge and brain areas controlling motoric side-effects. These experimental data in rodent and human tissue are consistent with the antiepileptic and motoric profile of perampanel in patients with refractory partial seizures. These data add to the growing body of data implicating that dampening of excitatory neurotransmission through AMPA receptors is a safe and effective means of seizure control. The introduction of perampanel (Fycompa) to the clinic will enable the opportunity for the first time to evaluate this mechanism compared to others in epilepsy therapeutics.

Acknowledgements

We thank the patient and his parents for their consent and contribution of cortical and hippocampal tissues to this research. We are grateful for their courage and generosity.

We also thank Randy Hunter, Mario Sgro, Deah Modlin, Brain Spegal, and Elizabeth Eberle, of Covance for their excellent work in carrying out the studies with intravenous PTZ, mouse electroshock, and rat amygdala kindling.

Author Contributions

Participated in research design: JM Witkin, X Ping, R Zwart, E Sher, SD Gleason, J Hobbs, and JL Smith

Conducted experiments: JM Witkin, SN Valli, X Ping, X Jin, R Zwart, E Sher, SD Gleason, J Hobbs, and JL Smith

Contributed new reagents or analytic tools: PJ Hahn, K Gardinier, D Gernert, JL Smith

Performed data analysis: JM Witkin, X Ping, R Zwart, E Sher, SD Gleason, PJ Hahn, K Gardinier, D Gernert, J Hobbs

Wrote or contributed to the writing of the manuscript: JM Witkin, X Ping, X Jin, R Zwart, E Sher, JR Sims, Jr, AS Chappell, SD Gleason, PJ Hahn, K Gardinier, D Gernert, J Hobbs, and JL Smith

References

Bak P (1996) *How Nature Works: the Science of Self-Organized Criticality.* Copernicus, New York.

Beggs JM (2008) The criticality hypothesis: how local cortical networks might optimize information processing. *Philos Transact A Math Phys Eng Sci,* **366:** 329-343.

Beggs JM and Plenz D (2003) Neuronal avalanches in neocortical circuits. *J Neurosci* **23**: 11167-11177.

Beggs JM and Plenz D (2004) Neuronal avalanches are diverse and precise activity patterns that are stable for many hours in cortical slice cultures. *J Neurosci* **24**: 5216-5229.

Brines ML, Sundaresan S, Spencer DD, and de Lanerolle NC (1997) Quantitative autoradiographic analysis of ionotropic glutamate receptor subtypes in human temporal lobe epilepsy: up-regulation in reorganized epileptogenic hippocampus. *Eur J Neurosci* **9**: 2035-2044.

Ceolin L, Bortolotto ZA, Bannister N, Collingridge GL, Lodge D, and Volianskis A (2012) A novel anti-epileptic agent, Perampanel, selectively inhibits AMPA receptor-mediated synaptic transmission in the hippocampus. *Neurochem Int* **61**: 517-522.

Chappell AS, Sander JW, Brodie MJ, Chadwick D, Lledo A, Zhang D, Bjerke J, Kiesler GM, and Arroyo S (2002) A crossover, add-on trial of talampanel in patients with refractory partial seizures. *Neurology* **58**: 1680-1682.

Cokic B and Stein V (2008) Stargazin modulates AMPA receptor antagonism. N*europharmacology* **54:** 1062-1070.

Della-Morte D and Rundek T (2012) Dizziness and vertigo. *Front Neurol Neurosci* **30**: 22-25.

Eusebi, F, Palma E, Amici M and Miledi R (2009) Microtransplantation of ligand-gated receptor channels from fresh or frozen nervous tissue into Xenopus oocytes: A tool for expanding functional information. *Prog. Neurobiol* **88:** 32-42.

French JA, Krauss GL, Biton V, Squillacote D, Yang H, Laurenza A, Kumar D, Rogawski MA (2012) Adjunctive Perampanel for refractory partial-onset seizures: randomized phase III study 304. *Neurology* **79**: 589-596.

Gao L, Xia L, Zhao FL and Li SC (2013) Clinical efficacy and safety of the newer antiepileptic drugs as adjunctive treatment in adults with refractory partial-onset epilepsy: a meta-analysis of randomized placebo-controlled trials. *Epilepsy Res* **103**: 31-44.

Hanada T, Hashizume Y, Tokuhara N, Takenaka O, Kohmura N, Ogasawara A, Hatakeyama S, Ohgoh M, Ueno M and Nishizawa Y (2011) Perampanel: A novel, orally active, noncompetitive

AMPA-receptor antagonist that reduces seizure activity in rodent models of epilepsy. *Epilepsia* **52**: 1331–1340.

Hayashi T (1952) A physiological study of epileptic seizures following cortical stimulation and its application to human clinics. *Japan J Physiol* **3**: 46-64.

Hibi S, Ueno K, Nagato S, Kawano K, Ito K, Norimine Y, Takenaka O, Hanada T, and Yonaga M (2012) Discovery of 2-(2-oxo-1-phenyl-5-pyridin-2-yl-1,2-dihydropyridin-3-yl)benzonitrile (Perampanel): a novel, noncompetitive α-amino-3-hydroxy-5-methyl-4-isoxazolepropanoic acid (AMPA) receptor antagonist. *J Med Chem* **55**: 10584-10600.

Hobbs JP, Smith JL, and Beggs JM (2010) Aberrant neuronal avalanches in cortical tissue removed from juvenile epilepsy patients. *J Clin Neurophysiol* **27**: 380-386.

Kato AS, Gill MB, Yu H, Nisenbaum ES and Bredt DS (2010) TARPs differentially decorate AMPA receptors to specify neuropharmacology. *Trends Neurosci* **33**: 241-248.

Krauss GL, Serratosa JM, Villanueva V, Endziniene M, Hong Z, French J, Yang H, Squillacote D, Edwards HB, Zhu J, and Laurenza A (2012) Randomized phase III study 306: adjunctive Perampanel for refractory partial-onset seizures. *Neurology* **78**: 1408-1415.

Krauss GL, Perucca E, Ben-Menachem E, Kwan P, Shih JJ, Squillacote D, Yang H, Gee M, Zhu J, and Laurenza A (2013) Perampanel, a selective, noncompetitive α-amino-3-hydroxy-5-methyl-4-isoxazolepropionic acid receptor antagonist, as adjunctive therapy for refractory partial-onset seizures: interim results from phase III, extension study 307. *Epilepsia* 2013 **54**: 126-134.

Lerche H, Shah M, Beck H, Noebels J, Johnston D and Vincent A (2013) Ion channels in genetic and acquired forms of epilepsy. *J Physiol* **591**(Pt 4): 753-764.

Löscher W and Nolting B (1991) The role of technical, biological and pharmacological factors in the laboratory evaluation of anticonvulsant drugs. IV. Protective indices. *Epilepsy Res* **9**: 1-10.

Mackenzie L, Medvedev A, Hiscock JJ, Pope KJ, and Willoughby JO (2002) Picrotoxin-induced generalised convulsive seizure in rat: changes in regional distribution and frequency of the power of electroencephalogram rhythms. *Clin Neurophysiol* **113**: 586-596.

Menuz K, Stroud RM, Nicoll RA, and Hays FA (2007) TARP auxiliary subunits switch AMPA receptor antagonists into partial agonists. *Science* 318: 815-817.

Miledi R, Palma E, and Eusebi F (2006) Microtransplantation of neurotransmitter receptors from cells to *Xenopus* oocyte membranes. New procedure for ion channel studies. *Meth Mol Biol* **322**: 342-355.

Palma E, Roseti C, Maiolino F, Fucile S, Martinello K, Mazzuferi M, Aronica E, Manfredi M, Esposito, V, Cantore G, Miledi R, Simonato M, and Eusebi F (2007) GABAa-associated rundown of temporal lobe epilepsy is associated with repetitive activation of GABAa "phasic" receptors. *Proc Natl Acad Sci USA* **104**: 20944-20948.

Palma E, Spirelli G, Torchia G, Martinez-Torres A, Ragozzino D, Miledi R, and Eusebi F (2005) Abnormal GABAa receptors from the human epileptic hippocampal subiculum microtransplanted to *Xenopus* oocytes. *Proc Natl Acad Sci USA* **102**: 2514-2518.

Palomero-Gallagher N, Schleicher A, Bidmon HJ, Pannek HW, Hans V, Gorji A, Speckmann EJ, and Zilles K (2012) Multireceptor analysis in human neocortex reveals complex alterations of receptor ligand binding in focal epilepsies. *Epilepsia* **53**: 1987-1897.

Rektor I, Krauss GL, Bar M, Biton V, Klapper JA, Vaiciene-Magistris N, Kuba R, Squillacote D, Gee M, and Kumar D (2012) Perampanel Study 207: long-term open-label evaluation in patients with epilepsy. *Acta Neurol Scand* **126**: 263-269.

Rektor I (2013) Perampanel, a novel, non-competitive, selective AMPA receptor antagonist as adjunctive therapy for treatment-resistant partial-onset seizures. *Expert Opin Pharmacother* **14**: 225-235.

Rogawski MA (2011). Revisiting AMPA receptors as an antiepileptic drug target. *Epilepsy Curr*. **11:** 56-63.

Rheims S, Ryvlin P (2013) Profile of perampanel and its potential in the treatment of partial onset seizures. *Neuropsychiatr Dis Treat* **9**: 9629-9637.

Rogawski MA (2013) AMPA receptors as a molecular target in epilepsy therapy. *Acta Neurol Scand* **127** (suppl 197): 9-18.

Rogawski MA and Hanada T (2013) Preclinical pharmacology of perampanel, a selective non-competitive AMPA receptor antagonist. *Acta Neurol. Scand* **127**(suppl. 197): 19-24.

Russo E, Gitto R, Citraro R, Chimirri A, and De Sarro G (2012) New AMPA antagonists in epilepsy. *Expert Opin Investig Drugs* **21**: 1371-1389.

Salman MS (2002) The cerebellum: it's about time! But timing is not everything--new insights into the role of the cerebellum in timing motor and cognitive tasks. *J Child Neurol* **17**: 1-9.

Schiff SJ, Jerger K, Duong DH, Chang T, Spano ML, and Ditto WL (1994) Controlling chaos in the brain. *Nature* **370**: 615-620.

Steinhoff BJ, Ben-Menachem E, Ryvlin P, Shorvon S, Kramer L, Satlin A, Squillacote D, Yang H, Zhu J, and Laurenza A (2013) Efficacy and safety of adjunctive Perampanel for the treatment of refractory partial seizures: A pooled analysis of three phase III studies. *Epilepsia* **54**: 1481-1489.

Stühmer W (1998) Electrophysiologic recordings from *Xenopus* oocytes. *Meth Enzymol* **293:** 380-300.

Tomita S, Chen L, Kawasaki Y, Petralia RS, Wenthold RJ, Nicoll RA, and Bredt DS (2003) Functional studies and distribution define a family of transmembrane AMPA receptor regulatory proteins. *J Cell Biol* **161**: 805-816.

Wirth C and Luscher HR (2004) Spatiotemporal evolution of excitation and inhibition in the rat barrel cortex investigated with multielectrode arrays. *J Neurophysiol* **91**: 1635-1647.

Wu JY, Guan L, and Tsau Y (1999) Propagating activation during oscillations and evoked responses in neocortical slices. *J Neurosci* **19**: 5005-5015.

Zaccara G, Giovannelli F, Cincotta M, and Iudice A (2013) AMPA receptor inhibitors for the treatment of epilepsy: the role of Perampanel. *Expert Rev Neurother* **13***:* 647-655.

Footnotes

[1]We thank the Pence family for supporting this work by a Pence foundation grant awarded to Jodi L. Smith.

Legends for Figures

Figure 1. Structure of the non-competitive AMPA receptor antagonist perampanel ([2-(2-oxo-1-phenyl-5-pyridin-2-yl-2,2-dihydropyridin-3-yl)benzonitrile hydrage 4:3]; Fycompa®).

Figure 2. Blocking effects of perampanel on native rat and human AMPA receptors from hippcampus and cerebellum microtransplanted into *Xenopus* oocytes. **A)** Example traces from oocytes injected with rat hippocampal (RH), rat cerebellar (RC), human hippocampal (HH), and human cerevellar (HC) membranes. AMPA receptors were activated by applying 100 μM AMPA and 100 μM CTZ to the oocytes. After 30 s of AMPA + CTZ application the valve of the perfusion system was switched to a solution that in addition to AMPA and CTZ also contained 30 μM perampanel (PRP). 30 μM perampanel inhibited the AMPA responses almost completely in all cases. **B)** Concentration-inhibition curves for perampanel on hippocampal (red 5curves) and cerebellar (black curves) AMPA responses. The protocol used was similar as shown in the traces above, except that in this case a range of different concentrations of perampanel were applied after the first 30 s of 100 μM AMPA + 100 μM CTZ application. Data are expressed as the mean ± SEM. The data were fitted with the Hill equation and the estimated values for IC_{50} and nH are shown in Table 1.

Figure 3. Antagonism by perampanel of human hippocampal membrane AMPA receptors from a 13-year old epileptic patient. Data are expressed as the mean ± SEM.

Figure 4. Description of dependent measures in the slice electrophysiological recordings.

A. Electrode array and data representation. Rat cortical tissue on the 60-channel micro-electrode array. An image from beneath the tissue is super imposed on top showing the electrodes that appear as small black circles at the ends of lines. Inter electrode distance is 200 μm and electrode diameter is 30 μm. Local field potential (LFP) signals on electrodes at one time step. Note that LFPs can vary in amplitude. A threshold of 3 standard deviations is applied to the recording. Supra-threshold LFPs are represented by small black squares.

B. **Example of an avalanche.** Seven frames are shown, where each frame represents activity on the electrode array during one 4 ms time step. Supra-threshold activity at electrodes is shown by small black squares. An avalanche is a series of consecutively active frames that is preceded by and terminated by blank frames. Avalanche length is given by the number of active frames, while avalanche size is given by the total number of active electrodes. The avalanche shown here has a length of 5 and a size of 9.

Figure 5. Effects of perampanel on amplitude and firing rate from cortical slice recordings from epileptic brain. Data are expressed as the mean ± SEM.

A. The average amplitude of each channel is plotted in microvolts. Perampanel (yellow) decreased the amplitude significantly, and the amplitude of the events did not recover during washout.

B. The average firing rate is plotted for each channel in Hz. Similar to the reduction in amplitude, perampanel significantly decreased firing rate activity which did not recover during wash-out.

Figure 6. Effects of perampanel on the branching parameter in the electrode array.

JPET Fast Forward. Published on July 15, 2014 as DOI: 10.1124/jpet.114.212779
This article has not been copyedited and formatted. The final version may differ from this version.

Table 1. Efficacy and Side-Effect Profile Quantification for perampanel and lacosamide (or diazepam).

Assay	Perampanel	Lacosamide
PTZ Clonus- rat	10.6 (4.1-49), p.o.	19.4 (8.1-64), i.p.
PTZ Seizure Threshold - rat	Not Effective up to 30, p.o.	Diazepam: 12.9 (8.1-28.9), i.p.
Inverted Screen- rat	3.8 (1.3-5.2), p.o.	19.7 (16.3-23.1), i.p.
PTZ Clonus - mouse	ED_{50} = 13.5 (2.2-46), i.p.	5.0 (3.2-6.7), i.p.
Inverted Screen- mouse	6.0 (1.9-10.8), ip	18.6 (15.8-21.4), i.p.
Electroshock - mouse (tonic extension)	1.7 (0.6-2.9), i.p.	Diazepam: 1.5 (0.8-2.6), i.p.
Amygdala Kindling rat – After Discharge Threshold	20.6 (6.8-32.1), p.o.	12.9 (7.3-24.5), p.o.
Amygdala Kindling rat – After Discharge Duration	MED >30, p.o.	MED >30, p.o.
Amygdala Kindling rat – Seizure Severity	MED = 30, p.o.	MED = 10, p.o.
Amygdala Kindling rat – 400 µA Stimulation	MED = 30, p.o.	MED >30, p.o.

Data are expressed as mg/kg. Data are given as ED_{50} (95% conf. limits). Values are from n=6-12 mice or rats.
All other data are minimal effective doses (MED). MED values are presented when the dose-effect functions did not permit calculation of ED_{50}.

JPET Fast Forward. Published on July 15, 2014 as DOI: 10.1124/jpet.114.212779
This article has not been copyedited and formatted. The final version may differ from this version.

Table 2. Effects of perampanel on native human and rat hippocampal and cerebellar AMPA receptors microtransplanted into *Xenopus* oocytes

Perampanel	**Human Hippocampus**	**Human Cerebellum**	**Rat Hippocampus**	**Rat Cerebellum**
IC50 (μM)	4.3 (3.9 - 4.8)	5.8 (5.4 - 6.3)	2.8 (2.2 - 3.6)	2.6 (1.5 - 4.8)
nH	1.15 +/- 0.05	1.07 +/- 0.04	1.55 +/- 0.23	1.31 +/- 0.35
Bottom (%)	0	0	7 +/- 5	3 +/- 10

Reported values are the mean ± SEM for nH and Bottom, and the mean with 95% confidence intervals for IC_{50}. For each group n=3. Dunnett's test analysis of log IC_{50} values did not reveal differences between human hippocampus and human cerebellum; rat hippocampus and rat cerebellum; human hippocampus and rat hippocampus, and human cerebellum and rat cerebellum (all p values > 0.05).

- Figure 1 -

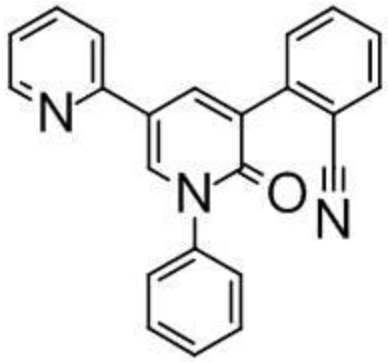

Figure 2.

a.

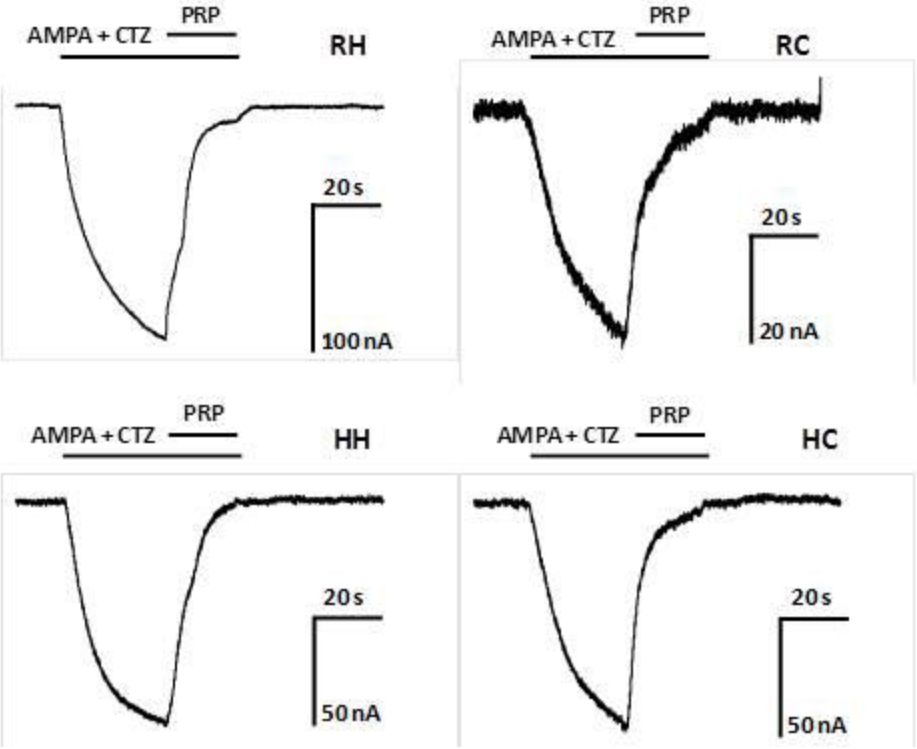
AMPA + CTZ
PRP
RH
20 s
100 nA
AMPA + CTZ
PRP
RC
20 s
20 nA
AMPA + CTZ
PRP
HH
20 s
50 nA
AMPA + CTZ
PRP
HC
20 s
50 nA

b.

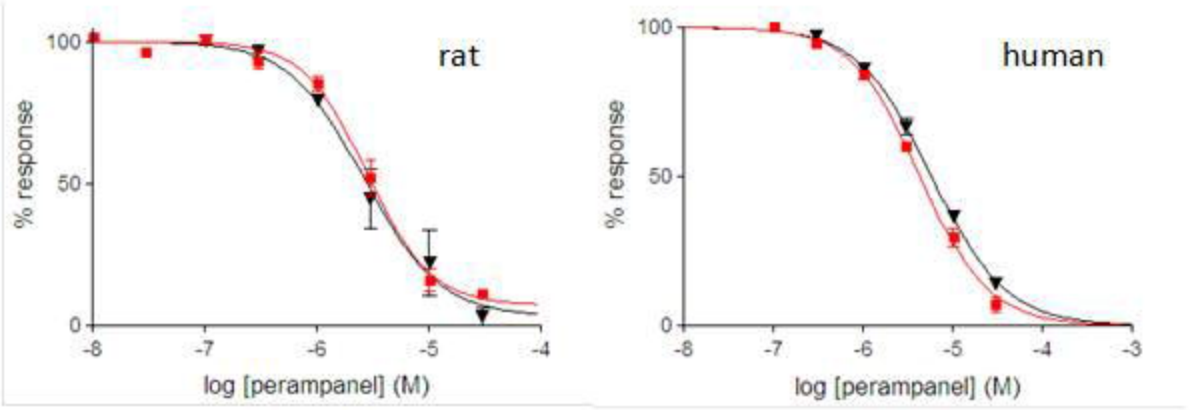
rat
% response
100
50
0
-8
-7
-6
-5
-4
log [perampanel] (M)
human
% response
100
50
0
-8
-7
-6
-5
-4
-3
log [perampanel] (M)

Figure 3.

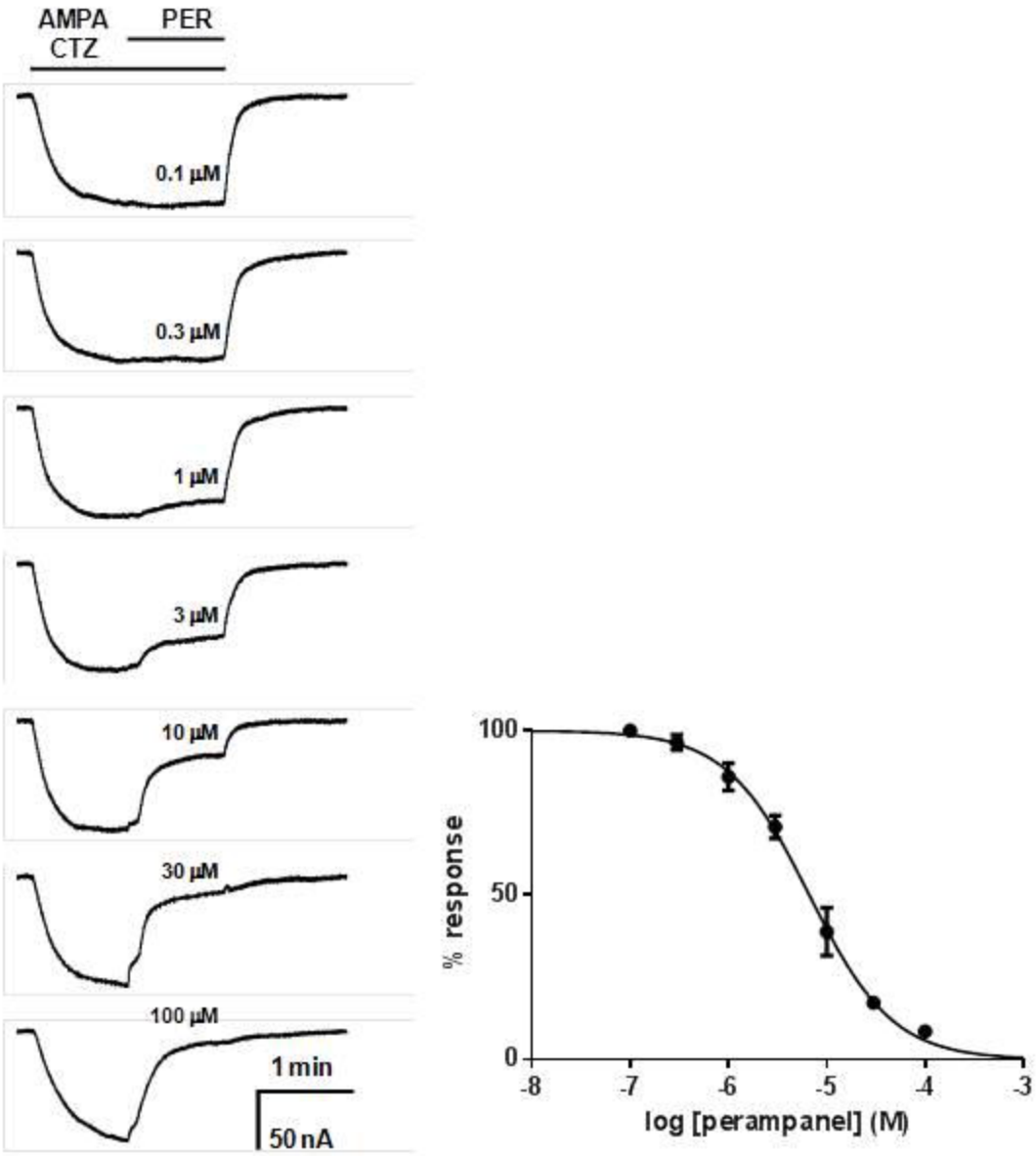
AMPA
CTZ
PER
0.1 µM
0.3 µM
1 µM
3 µM
10 µM
30 µM
100 µM
1 min
50 nA
100
50
0
% response
-8
-7
-6
-5
-4
-3
log [perampanel] (M)

JPET/2014/212779

- Figure 4 -

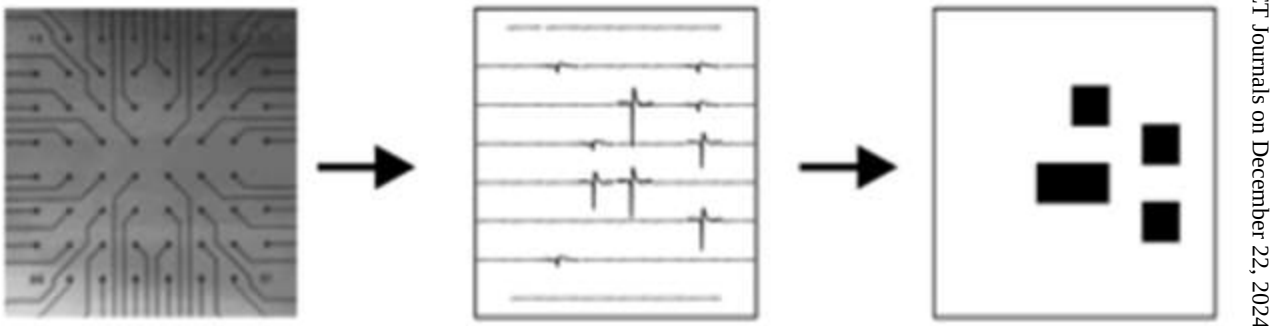

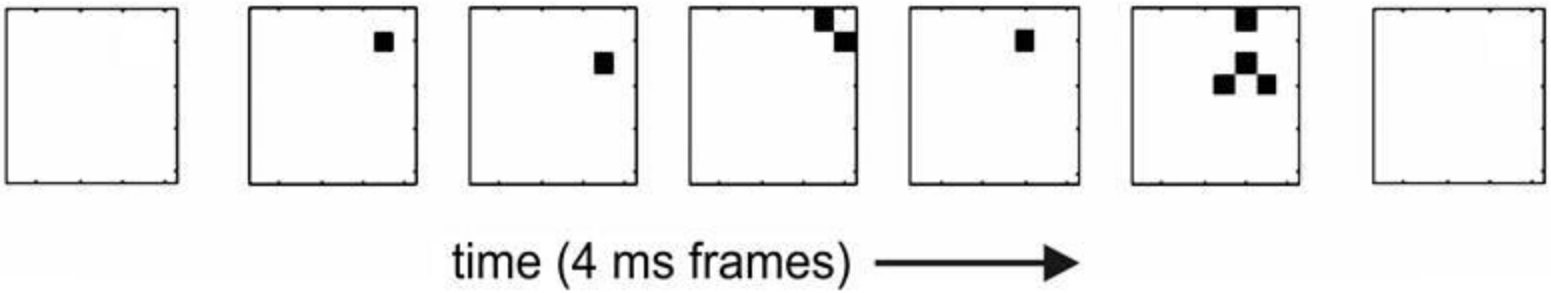

JPET/2014/212779

- Figure 5-

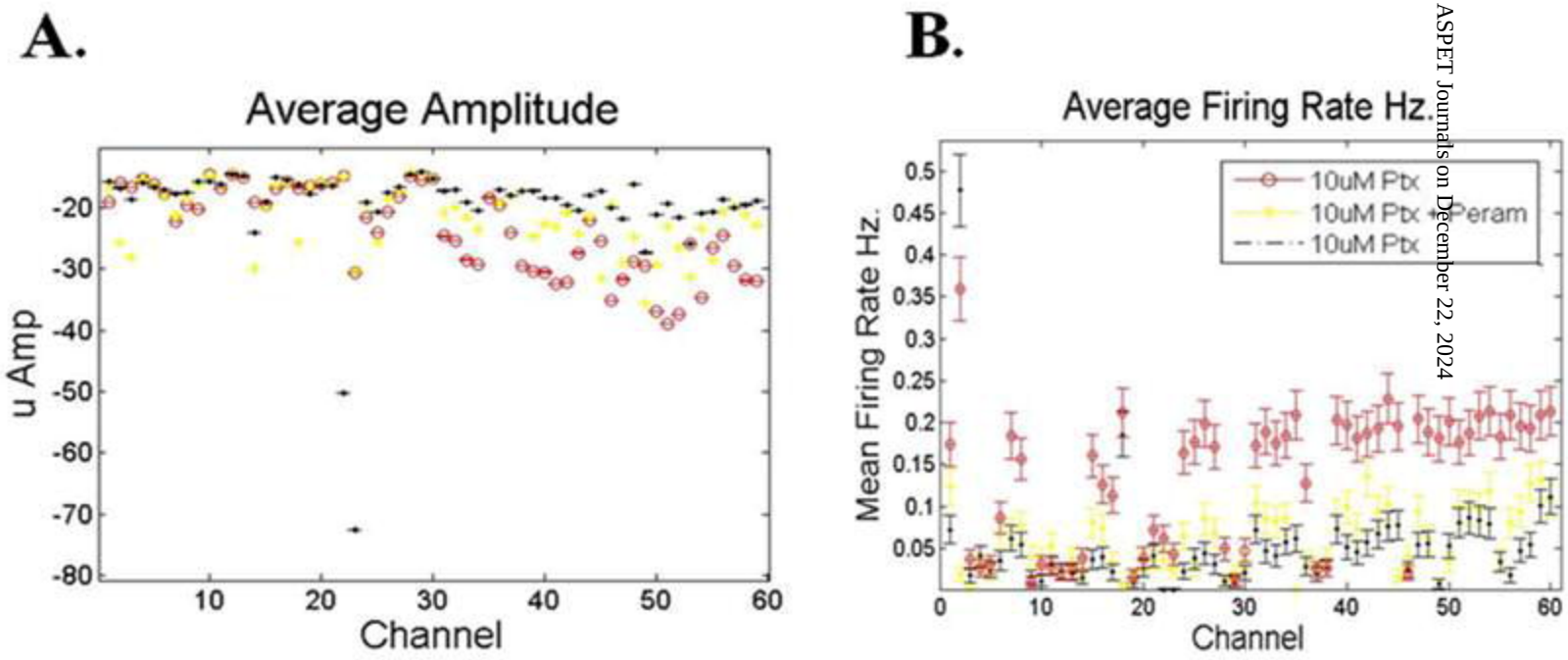

JPET/2014/212779

- Figure 6-